

Measurement of CO₂ Uptake Capacity in Source Rock Shales for GCS

Jin-Hong Chen^{1,*}, Amy J. Cairns¹, Stacey M. Althaus¹, and J. David Broyles¹

¹Aramco Americas: Aramco Research Center-Houston

Abstract. Geologic Carbon Sequestration (GCS) is an indispensable solution to reduce anthropogenic carbon dioxide (CO₂) in the atmosphere. Unconventional source rock shale reservoirs continue to gain momentum as a promising alternative to more conventional choices as potential GCS storage in our industry. To determine the suitability of an underground reservoir for GCS, the prospective ultimate storage or uptake capacity for CO₂ must first be estimated. This study analyzes the CO₂ storage mechanisms in organic-rich source rocks and determines a fit-for-purpose core analysis method for this application. A suitable core measurement method is dependent on the rock properties and the types of CO₂ storage mechanisms at play in the targeted formation. To quantitatively estimate the CO₂ storage in a reservoir, preserved core samples containing *in situ* fluids must be used. Importantly, all storage mechanisms associated with the rock must be accounted for, explicitly, CO₂ in the pore bulk (free gas), CO₂ adsorbed on the large pore surface (adsorbed gas), and CO₂ absorbed in the kerogen matrix and *in situ* pore fluids. CO₂ storage in nanoporous shale formations has been assessed using traditional volumetric and/or gravimetric adsorption analyses, albeit these methods are best suited for the characterization of homogeneous dry porous materials particularly in the form of powders or pellets. To address these limitations, we proposed and developed a specialized method to measure the CO₂ uptake capacity of intact preserved core samples with *in situ* fluids using high-field ¹³C nuclear magnetic resonance (NMR) spectroscopy using a custom designed high-pressure overburden cell. This paper analyzes and presents the measurement methods for quantifying CO₂ uptake capacity in source rock shales for GCS.

1 Introduction

Unconventional source rock shales significantly contribute to petroleum production worldwide, with the United States being the most important player producing approximately 10 Mb/d of oil and 100 Bcf/D of gas (US EIA Drilling Productivity Report, Feb. 2024). Suitable shale reservoirs located deep underground are also being investigated as viable CO₂ storage sites for Geologic Carbon Sequestration (GCS) as they have the potential to provide a safe and scalable pathway for permanent CO₂ storage (1-3). The ultra-small permeability of source rocks for CO₂ injection, comparing to conventional reservoirs, may be compensated by high well density, long horizontal length, and widespread hydraulic fractures in the formation, all of which have already been developed for hydrocarbon production from these reservoirs. Additionally, the chemical and physical properties of ultra-tight reservoirs naturally hinder the mobility of injected CO₂ thereby minimizing potential leakage. This is in contrast to aquifer and/or depleted conventional hydrocarbon reservoirs where caprock integrity is of paramount concern for long-term CO₂ storage.

The selection of candidate reservoirs for GCS is critically dependent upon having an accurate estimate of

the prospective ultimate storage capacity for injected volumes of CO₂. Existing methods for unconventional source rock reservoirs have relied on experimental techniques commonly used in materials science to characterize porous solids (e.g. activated carbons, zeolites, metal-organic frameworks, organic polymers, etc.) including physical adsorption and dynamic breakthrough measurements (4-6, 2, 7, 8). While these methods do offer insights into the gas sorption properties of source rock formations, caution must be taken when making assumptions in calculations and in material preparation. As such procedures can introduce uncertainty into the measurement that are not representative of intact core samples. For example, literature reports on the adsorption behavior of source rocks primarily include the analysis of powdered, cleaned, and dried samples. The samples are routinely subjected to solvent extraction and thermal treatment prior to sorption analysis since it is well-documented that moisture content can profoundly impact the gas sorption of porous materials (9). Importantly, in the context of subsurface CO₂ storage, analyzing cleaned and dried samples certainly lead to incorrect results since the source rock formation contains *in situ* fluids. Literature reports also documented the use of modeling methods to estimate GCS in source rock reservoirs, where CO₂ uptake capacity have been

* Corresponding author: JinHong.Chen@aramcoamericas.com

estimated using numerical simulations and then projected to full scale field scenarios (10, 11). The experimental and modeling methods lead to several orders of magnitude variances in the estimated storage capacities among the studies (1, 12, 6, 10, 2, 11, 13).

The CO₂ uptake capacity of a source rock reservoir should be estimated using intact samples that are in the original reservoir state with *in situ* fluids present. Pretreatment of samples by chemical extraction and/or thermal treatment must therefore be avoided. The measurement method of choice depends on how the CO₂ resides in the rock material. Thus, all gas storage mechanisms in the heterogenous rock matrix must be taken into consideration. This represents a daunting task given that the pores can range in size from nano to micrometer scale and the pore networks are inherently complex with varying wettability (14, 15).

In this paper, we first review the traditional adsorption methods and gas storage mechanisms to demonstrate that traditional methods are insufficient to estimate the CO₂ uptake capacity for source rock reservoirs. We will then introduce a new high-field NMR spectroscopy method that enables the amount of CO₂ injected into an intact plug containing *in situ* fluids to be accurately determined irrespective of the CO₂ storage mechanisms. The measured results suggest that source rock reservoirs have immense capacity for GCS.

2 Absolute sorption in intact source rock plug

Here, a brief review of the physical adsorption analysis methods applied to characterize source rock samples is provided. The advantages and shortcomings are highlighted for using the methods to estimate the CO₂ uptake capacity on preserved source rock plugs with *in situ* fluids. A ¹³C NMR method is then presented.

2.1 Surface area in source rock shales

Unconventional source rock shale reservoirs are fine-grained sedimentary rock, consisting of minerals intertwined with organic matter (16, 17), as shown by the scanning electron microscopy (SEM) image in Figure 1. The white and grey sections represent the mineral and kerogen, respectively, that forms the rock matrix. The much darker sections show the pores, which are associated with both kerogen and the mineral matrix (17). In this sample, and also in the majority of source rocks we have studied, the majority of pores are within the kerogen matrix.

As illustrated in Figure 1, pores in source rocks are generally on the nanometer scale, which results in a large total surface area. Figure 2 shows the estimated total surface area for a shale sample having a kerogen solid mass fraction of 10% ($f = 0.1$) and kerogen density of 1.3 g/cm³. The red and black curves represent the scenarios of 30% and 50% porosity in kerogen matrix, respectively. Details pertaining to the method and estimation can be found in Appendix A. As shown in Figure 2, one gram of material can easily exceed a total surface area of 10 m² for shale samples with an average pore size of 50 nm. In

contrast, the surface area is negligible for a conventional rock with pore sizes on the μm scale or larger. The higher surface area available for gas adsorption in source rocks is therefore a crucial parameter in estimating gas-in-place (18-20) and deemed important in estimating the potential CO₂ storage capacity.

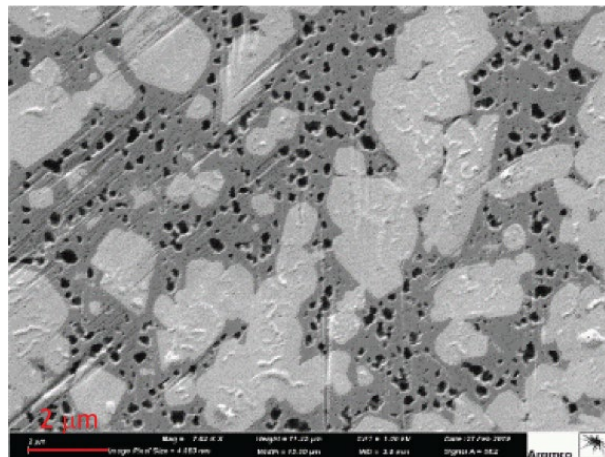


Fig. 1. SEM image of a representative source rock sample. The black, grey, and white colors illustrate the pore, kerogen, and mineral, respectively.

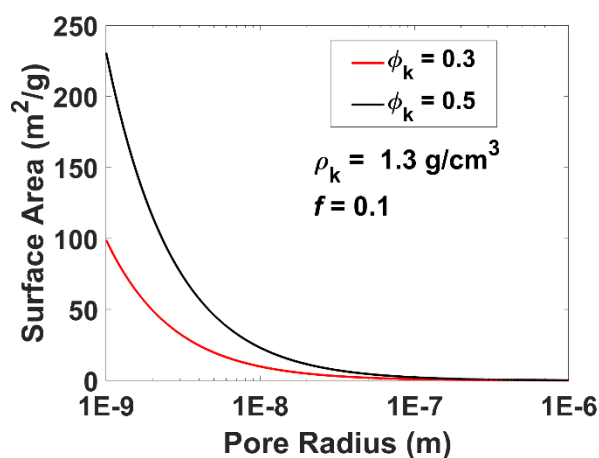


Fig. 2. Estimated total surface area for a source rock shale with 10% kerogen by weight and assuming the density of kerogen is 1.3 g/cm³. Refer to Appendix A for details on theory and method for estimation.

2.2 Adsorption characterization of porous materials: measurement methods

Adsorption is a surface process that refers to the adhesion or enrichment of molecules, atoms, or ions (adsorbate) to an interface (adsorbent) (21). In the case of a gas and solid system (e.g., porous material), adsorption takes place in the vicinity of the solid surface without penetrating the solid matrix as is the case in absorption. The adsorption process creates a film of the adsorbate on the adsorbent surface with a very different density from the related gas state, especially at low pressure. Adsorption is usually

described using isotherms, that is, the amount of adsorbate on the adsorbent as a function of its pressure at equilibrium and a constant temperature. The quantity adsorbed is normalized by the mass of the adsorbent to allow comparison of different materials. Langmuir was the first to derive a semi-empirical isotherm in 1918 (22) which has been the most common isotherm equation to use due to its simplicity and its ability to fit a variety of adsorption data.

Adsorption at the gas-solid interface is routinely measured in the laboratory (21). As adsorption occurs at the interface, the weight of the solid increases and the pressure of the gas decreases. This allows two approaches to measure the amount adsorbed on the surface:

- the change in weight of the solid with a mass balance (gravimetric method).
- the change in pressure of the gas in an accurately known volume, if the volume of the sample is also known (volumetric method).

Commercial instruments based on these two methods are available; but they only measure the excess adsorption of single or multi-component gases. Excess adsorption is the difference between the amount of measured gas and the amount of a reference inert gas that would be present in the same sample in the absence of adsorption at the same temperature and pressure (23, 21). The accuracy of adsorption data critically relies on the correct determination of the void volume using an inert gas. This becomes increasingly important for materials with low uptake and small amount of available sample. Helium is generally selected for this purpose given its small kinetic diameter (0.265 nm) and inertness toward many types of materials.

These adsorption techniques and isotherm models have been the standard method reported in the literature for gas sorption analysis of source rock shales, irrespective of the gas used in the measurement (20).

2.3 Absorption and dissolution in preserved source rocks

The organic matter, kerogen, is a key polymeric component in source rocks, which can occupy a significant portion of the matrix volume, for example, approximately 50% for the sample shown in Figure 1. It has long been established that CO₂ and light hydrocarbons such as methane (CH₄) can be absorbed into the kerogen matrix, causing it to deform and swell (24-26, 7, 27).

Absorption is a physical or chemical phenomenon in which molecules, atoms, or ions penetrate the bulk phase of a material matrix. Figure 3 provides an illustration of the adsorption and absorption process for a small section of a pore with a solid matrix. Figure 3a shows the case of adsorption where molecules are in the free gas state in the bulk and adsorbed (ads.) state on the solid surface. Figure 3b shows the case where both adsorption (ads.) on the surface and absorption (abs.) in the matrix are present. The absorbed molecules in the solid can exchange with adsorbed gas and/or free gas molecules by the diffusion process.

Considering the large volume fraction of kerogen in source rocks, absorption of gas into the kerogen matrix can be a crucial factor in determining the total gas at any given pressure and temperature. Similarly, CO₂ absorption can also occur in clay minerals (28) and thus must be accounted for in shale samples with significant amounts of clay. Notably, the CO₂ adsorption behavior in clay minerals under reservoir conditions is not well understood according to literature reports (29).

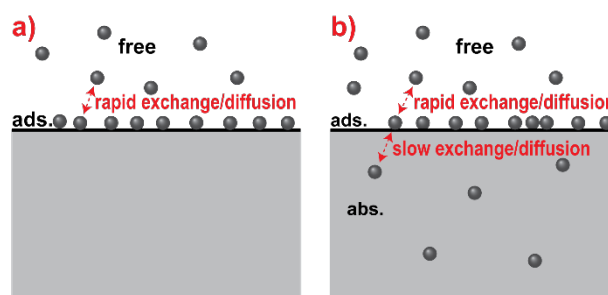


Fig. 3. Schematic to illustrate adsorption and absorption for a section of a solid (grey) with surface (black line). (a), adsorption only with molecules in free state in the bulk and adsorbed (ads.) on the solid surface. (b), both adsorption and absorption (abs.) with molecules in three different states. Molecules at different states are under dynamic equilibrium with rapid or slow exchange as in (a) and (b) at a given temperature and pressure.

Another important factor in estimating CO₂ uptake capacity in source rocks is the dissolution of CO₂ in the pore fluids. When injecting CO₂ into a depleted reservoir for storage, the porosity of the rock formation is partially filled with residual fluids which allow CO₂ dissolution. Core plugs from shale reservoirs contain large amounts of *in situ* fluids owing to the extremely low permeability and complex configuration of connected or isolated porosity that leads to fluid retention in the rocks (30, 31). For example, approximately 75% of fluids cannot be removed from Devonian shale samples using the Dean-Stark method (32). This limitation was in fact the motivation for developing the crushed rock analysis, or the now famous Gas Research Institute (GRI) method (32), for porosity measurements of shales. As aforementioned, appropriate laboratory methods to assess CO₂ uptake capacity in source rock reservoirs must be able to account for and handle the *in situ* fluids because a significant amount of CO₂ may become dissolved in the fluids.

In this study, the dissolution of gas in fluid is accounted for as one type of absorption. Therefore, absorption includes CO₂ adsorbed in kerogen matrix and dissolved in pore fluids.

2.4 Absolute sorption in a preserved source rock plug

To accurately assess the CO₂ uptake capacity in source rocks, experimental methods must consider all storage mechanisms at a given pressure and temperature under equilibrium conditions.

As outlined in sections 2.2 and 2.3, three storage mechanisms exist in organic-rich source rocks, thereby ensuring three different gas constituents:

- molecules in the pore-bulk or interior of the pores excluding those adsorbed on the pore surface.
- molecules adsorbed on the pore surfaces within the kerogen and minerals, which make up the excess adsorption in traditional adsorption analysis (21).
- molecules absorbed in the kerogen matrix and in the reservoir fluids.

Here, the total gas in a sample described by the three storage mechanisms is defined as “absolute sorption”, which also gives the uptake capacity of the sample for the studied gas because it is the ultimate quantity that can be stored in the sample at the given state.

Absorption of CO₂ in the kerogen matrix and pore fluids are competing mechanisms. Intrinsically, the absorption of gas in kerogen matrix leads to deformation and swelling of the kerogen which reduces the pore size and volume in the rock. Vice versa, CO₂ absorption in the pore fluids can increase its volume thereby impacting the kerogen matrix. At any given temperature and pressure, the amount of CO₂ in a sample is thus the result of a thermodynamic equilibrium of all storage mechanisms and competing interactions of injected CO₂, pore fluids, and kerogen matrix. Traditional adsorption analysis methods are ideally suited for the characterization of dry adsorbent materials that are rigid in nature, but we are of the opinion that this method falls short in providing an accurate assessment of the CO₂ absolute sorption in source rock samples containing a non-rigid kerogen matrix in presence of *in situ* fluids. We do however recognize the value of this application when it comes to comparing data to literature reports and for its ability to serve as a useful screening tool for rapid down-selection of rock samples for in-depth CO₂ uptake storage studies using the NMR technique.

3. Experimental methods

3.1 Samples

The process of restoring a source rock sample to the reservoir condition poses a significant challenge. To date, there is no agreement in the industry on best practices nor a standardized procedure and therefore preserved intact samples were used for this study. Briefly, the drilled whole core was surfaced from the downhole and preserved with three layers of wrapping including plastic wrap, aluminum foil, and wax. It was then shipped to the laboratory for the core plugging procedure. Note that a majority of the reservoir liquid remained in the preserved rock on the studied cores; whilst a portion of the light hydrocarbon phase was released from the core during surfacing from the reservoir due to changes in the surrounding pressure.

Slim cylindrical plugs were drilled from the whole core using a 3.5 mm diamond coring bit from Scorpion Engineering. The drilled slim plug was then polished on both ends to flat parallel surfaces. The liquid content in the plug was measured using a 12 MHz NMR spectrometer from Oxford Instruments (33) and found to exceed 10% of the rock volume, thereby indicating a large total pore fluid in the sample.

Samples were cut from the same section in the whole core as the slim plug and crushed to a desired particle size for volumetric high-pressure gas adsorption analysis.

3.2 High-pressure gas adsorption

High-pressure (HP) adsorption equilibrium measurements of pure CO₂ gas were performed using an iSORB dual-station HP series gas sorption system from Anton Paar Instruments. The volumetric gas sorption system is equipped with a gas reservoir with an internal volume of 100 cm³ for pressurized gas storage. A recirculator system was used to control the temperature (+/- 0.01°C) during adsorption analysis by securing dewars to the analysis ports.

For this set of measurements, rock samples were crushed to a particle size of 425 – 850 microns using a mortar and pestle and loaded into a pre-weighed stainless-steel microcell (AISI 316) having a unibody design and estimated volume of 2.6 cm³. A 2-micron filter was inserted on top of each cell to minimize elutriation. The samples were degassed by securing a mantle heater to the analysis ports and increasing the temperature in a stepwise fashion from room temperature to 80°C at a ramp rate of 2°C per minute and held constant for 1 h followed by heating to 110°C at a ramp rate of 5°C per minute and held for 12 h. Effective temperature was selected as the void volume mode given the analysis (80°C) and manifold (50°C) temperatures. In this work, the equation of state (EOS) used was the Helmholtz equation (34).

At the onset of this study, a null blank adsorption isotherm was measured under analogous temperature and pressure conditions using a microcell with an estimated volume of 2.6 cm³. The assigned sample weight was normalized to 1 gram to determine the CO₂ uptake in the empty vessel. This information was applied to the corrected excess isotherm using the instrument software to determine the helium (skeletal) density of the shale powder (adsorbent) as this is an input parameter along with bulk density needed to determine the storage capacity.

Additionally, a blank CO₂ adsorption isotherm was collected under analogous temperature and pressure conditions in the presence of inert stainless steel 316 beads. The purpose was to closely match the volume of the beads to that occupied by the adsorbent. Notably, in cases where the adsorption is too low, the background signal cannot be neglected. To remove the contribution of the background signal, the excess isotherm is corrected with a blank cell subtraction. Importantly, the corrected isotherm is used to determine the CO₂ storage capacity. The tapped (bulk) density, 1.39 g/cm³, was measured for the studied shale sample using an Auto Tapper apparatus as this is the other input parameter needed to calculate the CO₂ storage capacity.

3.3 ¹³C NMR spectroscopy method for CO₂ absolute sorption

In this section, we introduce a new specialized method using ^{13}C NMR spectroscopy to measure the absolute sorption of CO_2 in an intact source rock plug. To enhance the NMR sensitivity, ^{13}C labeled CO_2 is used in experiment.

The custom sample cell was specifically designed to withstand the experimental operating conditions and fit within the probe of the 500 MHz Bruker Aeon NMR spectrometer. Accordingly, the overburden cell (Daedalus Innovations), illustrated in Figure 4a, is made with zirconia of 5 mm OD and 3.69 mm ID. An NMR coil around the cell for detection is illustrated in Figure 4b. In a typical experiment, the drilled slim plug is loaded in the overburden cell. An inlet tube located at the top of the cell is used to apply vacuum in the cell to remove the air and for CO_2 injection into the cell, including the slim plug, as illustrated in Figure 4b.

The 1D ^{13}C NMR spectra were acquired at equilibrium states with pressure steps increasing from 0 to 4000 psi. The overburden cell and inlet line were first vacuumed for approximately 30 seconds, after which the ^{13}C chemical shift NMR spectrum was acquired. Afterwards, ^{13}C labeled CO_2 (Cambridge isotopes) was injected to a set pressure, for example first at 100 psi, until an equilibrium state was reached. A ^{13}C NMR spectrum was again acquired. The experiment was repeated at the next set pressure and so forth up to 4000 psi. The overburden cell was maintained at 40°C for all the experiments.

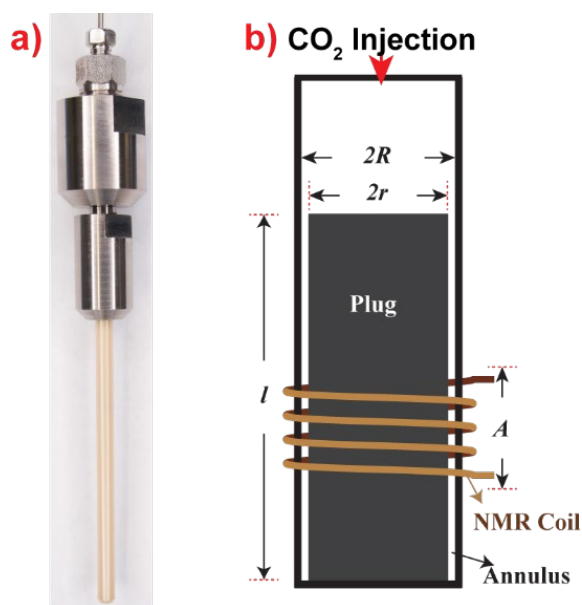


Fig. 4. Overburden cell (a) and illustration of the plug in the cell (b) for CO_2 injection and ^{13}C NMR measurement at 500 MHz.

4 Results and discussion

4.1 High-pressure adsorption for source rock powder

Adsorption measurements for shale samples can provide some insight toward assessing the CO_2 sequestration potential of geological formations. Analytical methods for

measuring gas adsorption, whether gravimetric or volumetric, experimentally measure the excess adsorption (23, 21), as aforementioned in section 2.2. The storage capacity of CO_2 for a source rock sample is the summation of the measured excess sorption and gas in the pore-bulk.

Figure 5 shows the measured CO_2 storage capacity at 80°C and pressures up to 1100 psi for a crushed source rock. The experiment was repeated three times to evaluate the isotherm reproducibility, as denoted by Runs 1-3 in Figure 5. Notably, the sample was not removed from the instrument, instead the isotherm was collected, then the sample was degassed, and the process repeated.

As discussed previously, adsorption analysis of powdered source rock sample is not a true representation because gas absorbed in the kerogen matrix and pore fluids would be counted as surface adsorption in the process, i.e., the measured excess sorption would include the absorbed gas. Therefore, reference in the context of this specific application the obtained net values in Figure 5 from the traditional technology can only be used as a reference. This method does however provide a quick high-throughput approach to pinpoint general trends by making comparisons across samples. The result is used to select slim plugs for the following NMR measurement.

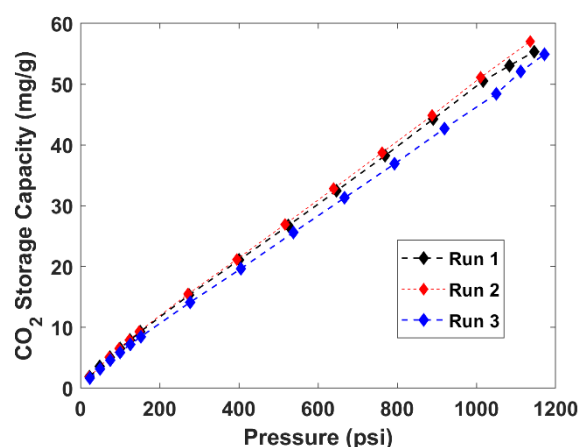


Fig. 5. Estimated CO_2 storage capacity for a crushed shale sample. Isotherms were collected at 80°C using the volumetric adsorption method. Testing was repeated three times on the same sample.

4.2 CO_2 uptake capacity of source rocks from high-field ^{13}C NMR

4.2.1 NMR spectrum and deconvolution

A standard NMR spectrum measures all the ^{13}C spins within the NMR detection coil with an axial length A , as illustrated in Figure 4b (35, 36). In the absence of a plug in the overburden cell, the detected ^{13}C NMR signal comes only from CO_2 in the bulk state as evidenced by a single peak observed in the spectrum, shown in Figure 6a.

Figure 6b was the acquired ^{13}C spectrum with a plug in the overburden cell after 30 s under vacuum, which shows no observable signal. The plug contains more than 10% of liquid hydrocarbons by volume and

approximately 10% kerogen by weight. ^{13}C was not observed at the experimental condition mainly because the natural abundance of ^{13}C in both kerogen and liquid hydrocarbon is only 1.1%. Additional reasons include large linewidth from short transverse relaxation time and limited gyromagnetic ratio (^{13}C is only approximately $\frac{1}{4}$ of ^1H). The fact that there is no observable ^{13}C NMR signal from the kerogen matrix and hydrocarbon liquid is very beneficial to quantify the injected CO_2 in the plug because it alleviates the need to account for background signals.

In the presence of a plug in the overburden cell, CO_2 can be in the annulus and in the source rock plug. Figure 7a shows the ^{13}C spectrum acquired at 500 psi. The spectrum includes a sharp peak and a broad peak that partially overlap from the presence of CO_2 in the annulus and plug, respectively. The annulus measures approximately 0.1 mm and thus in this environment CO_2 behaves as if it were in the bulk state.

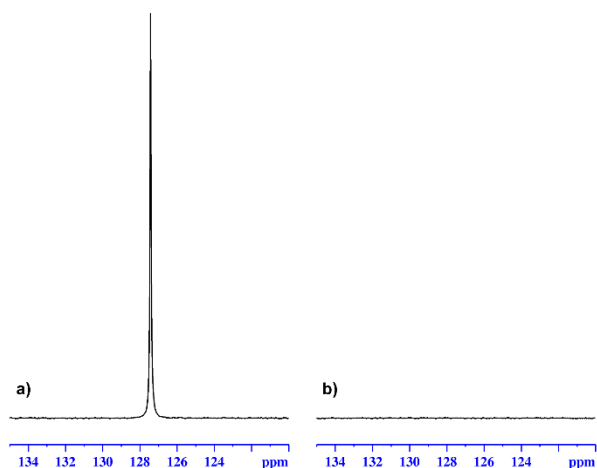


Fig. 6. ^{13}C NMR spectra of a) bulk CO_2 at 100 psi, b) a plug in the overburden-cell at 0 psi.

To quantify the amount of CO_2 from the spectral in Figure 7a, the ultimate task is to separate the NMR signal in the acquired spectrum from CO_2 in the annulus and in the plug, based on the NMR property of the two signals in different environments. The linewidth of an NMR peak is determined by the transverse relaxation time T_2 and inhomogeneity of the static field (35). The sharp peak in Figure 7a can be easily assigned to the bulk CO_2 in annulus and the broad peak to the CO_2 in the plug. Note that the NMR signals of CO_2 in the rock and in the bulk are resolved in the spectrum which allows for their easy separation and quantification, thereby rendering the NMR method unique and extremely useful for the current application. Traditional adsorption methods that relied on weight or volume measurements cannot distinguish gas in different environments and thus additional steps must be taken into account using reference cells with inert gas to obtain excess adsorption (21).

The large differences in linewidth and chemical shifts for the CO_2 in the plug and in the annulus in the ^{13}C

spectrum allow separation and quantification of the two signals. We used a deconvolution method by minimizing the least square of the measured spectrum and two Lorentzian peaks of different intensity, width, and chemical shift. The deconvolution result was shown in Figure 7b with the dashed green peak and red peak assigned to CO_2 in the annulus and plug, respectively. The dash-dotted blue line is the deconvolution error between the acquired NMR spectrum (black curve) and the summation of the two peaks (green and red curves). From the deconvolution, we obtained the integrals of the two peaks, among other parameters. The spin magnetizations M_0^{plug} and M_0^{an} of CO_2 in the plug and in the annulus are proportional to the integral of these two peaks.

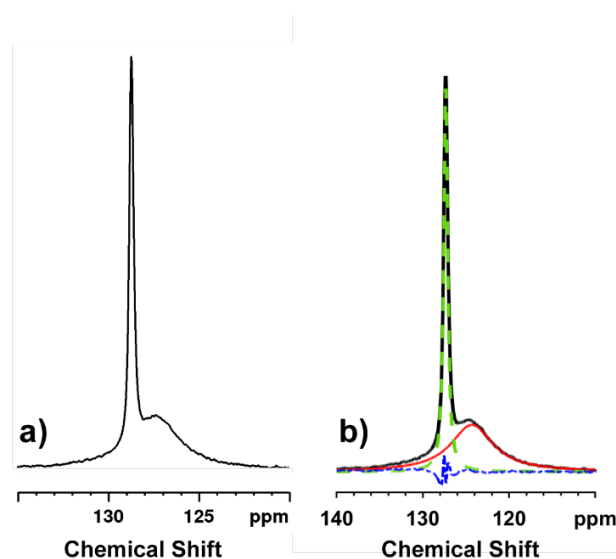


Fig. 7. a), ^{13}C spectra with a plug in the overburden cell at 500 psi. b), deconvolution of the ^{13}C spectrum in (a). The solid red and dashed green lines represent the CO_2 in the plug and in the annulus, respectively. The dash-dotted blue line is the deconvolution error.

We used the relative intensity of the $M_0^{\text{plug}} / M_0^{\text{an}}$ and the property of CO_2 in the annulus to obtain the absolute sorption of CO_2 in the plug. The amount of CO_2 in the annulus can be calculated from the volume of the overburden cell minus the plug volume and the density of CO_2 at the experimental pressure and temperature, as

$$M_0^{\text{an}} = c\pi(R^2 - r^2)A\rho \quad (1)$$

Where c is a constant converting the CO_2 mass to NMR magnetization, ρ is the CO_2 density in the bulk state at the experimental temperature and pressure which can be found from literature or from previous measurements. R and r are the inner radius of the overburden-cell and radius of the rock plug, respectively, and A is the aperture of the NMR detection coil, as illustrated in Figure 4b. The annulus signal can serve as a standard for quantification of CO_2 in the rock plug. Specifically, the acquired NMR signals of CO_2 in the plug and in the annulus are determined by the respective volume and density and we have,

$$\frac{M_0^{plug}}{M_0^{an}} = \frac{\pi r^2 A \phi \rho_p}{\pi (R^2 - r^2) A \rho} \quad (2)$$

where ρ_p is the average density of CO₂ in the pore system of the source rock shale. Because of the multiple sorption mechanism discussed in section 2, ρ_p can be very different from bulk density ρ . ϕ is the average volume fraction occupied by CO₂ over the entire rock volume. Considering the full cylindrical plug, the total CO₂ injected into the plug is

$$m_{pf} = \pi r^2 l \phi \rho_p \quad (3)$$

where l is the plug length. Combining Eqs. (2) and (3), the absolute sorption of CO₂ per unit rock mass is then obtained as

$$\frac{m_{pf}}{m_p} = \frac{\pi l (R^2 - r^2) \rho}{M_0^{an} / M_0^{plug} m_p} \quad (4)$$

where m_p is the measured plug mass. For the measured ¹³C spectrum in Fig. 7b at 500 psi and 40 °C, using the ratio from the deconvolution $M_0^{plug} / M_0^{an} = 1.43$, bulk density of CO₂ $\rho = 6.96 \times 10^{-5}$ g/mm³, and parameters about the sample and the overburden cell: $m_p = 1028.5$ mg, $l = 48.63$ mm, $R = 3.76$ mm, $r = 3.40$ mm, we obtained the absolute sorption of CO₂ in the plug is 7.93 mg/g of the rock.

¹³C NMR detects all the CO₂ in the source rocks, irrespective of where they reside and whether they have different properties in the pores, pore surface, and the composite matrices (organic and minerals) of the source shales. Thus, NMR directly detects the absolute sorption of CO₂ in the rock sample without the need to use equation of state, a reference gas, and other assumptions which can introduce uncertainties as mentioned earlier in the case of traditional physical adsorption methods.

All CO₂ adsorption and absorption from different constituents in the plug shows up in the spectrum as a single broad peak. This allows the estimation of a lower bound of CO₂ diffusion coefficients in kerogen. The timescale for each NMR measurement is on the order of 1 s. The diffusion resulted exchange time of CO₂ in the kerogen and in the pore should thus be much smaller than 0.1 s given that only one uniform peak was observed. Considering the diffusion distance L for a CO₂ molecule to the nearest pore is generally smaller than $L = 0.1$ μm in the studied sample, as shown by the SEM in Figure 1, the smallest diffusion coefficient of CO₂ in kerogen matrix, using Einstein diffusion equation, $D = L^2 / 6\tau$, is estimated to be 1.7×10^{-14} m²/s. Note that the diffusion coefficient could be much larger than this value.

4.2.2 CO₂ in annulus

As previously discussed, CO₂ in the annulus was used as a standard for quantification for CO₂ in the plug to avoid

involving additional internal or external standards which would complicate the experimental protocol. For easy use, we selected the bulk density at 4000 psi and 40 °C, $\rho = 896.02$ kg/m³, as a known value. This was then used to calculate the density at any other pressure for CO₂ in the annulus from the measured NMR signals.

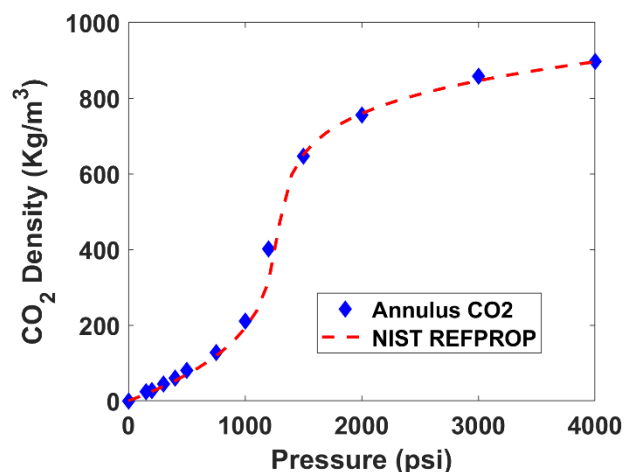


Fig. 8. NMR measured density isotherm of CO₂ in the annulus of a plug loaded in the overburden cell. The red dashed line is theoretical density calculated using NIST Refprop (37).

Figure 8 shows the comparison of an obtained density isotherm of CO₂ in the annulus using this method with the theoretical bulk density using NIST (National Institute of Standards and Technology) Software Refprop (37). The good consistency confirms that the CO₂ in the annulus can be treated as bulk state. It also shows that the proposed high-field NMR method is accurate.

4.2.3 CO₂ uptake capacity in source rock

Figure 9 shows the measured CO₂ absolute sorption in five plugs from two wells of the same source rock reservoir. Plugs A1 and A2 were from well A and separated by about 3 feet in vertical depth. Plugs B1, B2, and B3 were from well B and separated over 60 feet.

The CO₂ absolute sorption for all five plugs had similar uptakes at pressures up to 500 psi. After which, the isotherms started to diverge. The absolute sorption for the three samples from well B is sensitive to pressure in the range of 500 psi to about 1500 psi. After 2000 psi, the rate of increase is much smaller.

At 4000 psi, the storage capacity for well B plugs are 2 to 3 times greater than the plug from well A. Efforts are underway to gain a deeper understanding of this behavior and will be presented in the future. Nevertheless, the data clearly indicates that well B is a much better candidate for CO₂ injection for GCS.

The estimated CO₂ absolute sorption from the NMR measurement, allows us to estimate the potential uptake capacity of a source rock reservoir for GCS. The average CO₂ sorption of the five samples at 4000 psi is 42.9 mg/g. Accordingly, for a hypothetical source rock shale

reservoir of 100 km in length and width and 50 m in depth with an average density of $2.3 \times 10^3 \text{ kg/m}^3$, we can estimate the uptake capacity of the reservoir to be 4.92×10^{10} tons of CO_2 . Although this should be considered as the upper limit of the reservoir for CO_2 sequestration, the results indicate source rock shale reservoirs do have the capacity for large GCS.

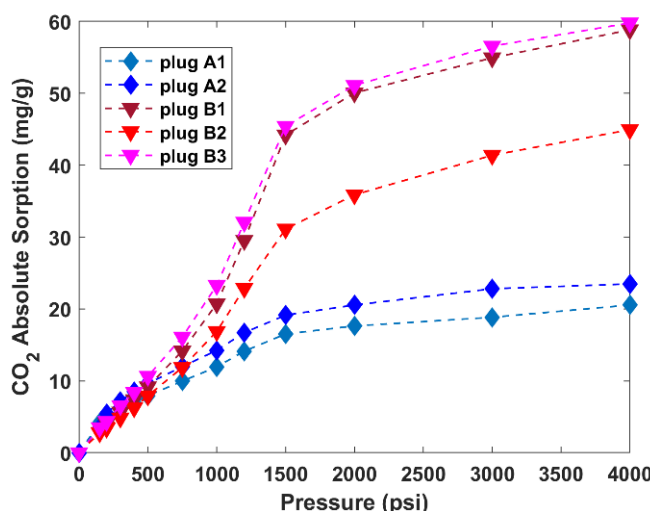


Fig. 9. NMR measured CO_2 absolute sorption isotherms for five plugs from two wells A and B.

5 Conclusion

This study attempts to determine a fit-for-purpose method to evaluate CO_2 uptake capacity in organic-rich source rocks. To estimate the CO_2 storage in a reservoir, preserved intact core samples containing *in situ* fluids must be used. Considering all possible CO_2 storage mechanisms in source rocks including CO_2 in the pore bulk (free gas), CO_2 adsorbed on the large pore surface (adsorbed gas), and CO_2 absorbed in the kerogen matrix and in the *in situ* pore fluids, traditional volumetric and/or gravimetric adsorption analyses cannot obtain correct CO_2 uptake capacity.

An NMR spectroscopy method was proposed and developed to measure uptake capacity of CO_2 in preserved intact source rock plugs. The method utilizes the NMR property difference in chemical shift and transverse relaxation time for CO_2 in the source rock and in the bulk state. The acquired ^{13}C NMR spectrum was decomposed to quantify the CO_2 in the annulus and in the plug. The NMR spectroscopy method does not require a conceptual *a priori* equation of state in nanopores nor the specific positioning and properties for CO_2 in the pores and matrix of source rock shale samples. It provides accurate results in the presence of *in situ* fluids in the sample with a non-rigid composite matrix.

The measured absolute sorption of CO_2 in the source rocks provided experimental data to assess the GCS capacity of the reservoirs. From the measured data, it was estimated a reasonable sized source rock shale reservoir can have a large GCS capacity.

References

1. R. W. J. Edwards, M. A. Celia, K. W. Bandilla, F. Doster, C. M. Kanno, *Environ. Sci. Technol.* **49**, 9222 (2015).
2. B. C. Nuttal, C. Eble, R. M. Bustin, J. A. Drahovzal, in *Greenhouse Gas Control Technologies 7*, E. S. Rubin *et al.*, Eds. (Elsevier Science Ltd, Oxford, 2005), pp. 2225.
3. L. Ribeiro, A. Thoma, J. Bryant, D. Sundararajan, W. Zurovec, in *SPE Hydraulic Fracturing Technology Conference and Exhibition*. (2022).
4. H. Aljamaan *et al.*, *Energy Fuels* **31**, 1193 (2017).
5. R. J. Ambrose, R. C. Hartman, M. Diaz-Campos, I. Y. Akkutlu, C. H. Sondergeld, in *SPE Unconventional Gas Conference*. (2010), vol. All Days.
6. B. Hazra, V. Vishal, C. Sethi, D. Chandra, *Energy Fuels* **36**, 9882 (2022).
7. D. J. K. Ross, R. M. Bustin, *Bulletin of Canadian Petroleum Geology* **55**, 51 (2007).
8. F. P. Wang, R. M. Reed, A. John, G. Katherine, in *SPE Annual Technical Conference and Exhibition*. (2009).
9. R. T. Woodward *et al.*, *J. Am. Chem. Soc.* **136**, 9028 (2014).
10. F. Liu, K. Ellett, Y. Xiao, J. A. Rupp, *Int. J. Greenhouse Gas Control* **17**, 111 (2013).
11. Z. Tao, A. Clarens, *Environ. Sci. Technol.* **47**, 11318 (2013).
12. M. L. Godec, H. Jonsson, L. Basava-Reddi, *Energy Procedia* **37**, 6656 (2013).
13. H. Vidas, R. Hugman, C. Clapp, *Energy Procedia* **1**, 4281 (2009).
14. J.-H. Chen *et al.*, in *SPWLA 53rd Annual Logging Symposium*. (Cartagena, Colombia, 2012), vol. All Days.
15. R. G. Loucks, R. M. Reed, S. C. Ruppel, U. Hammes, *AAPG Bulletin* **96**, 1071 (2012).
16. Y. N. Abousleiman *et al.*, *Acta Geotech.* **11**, 573 (2016).
17. R. G. Loucks, R. M. Reed, S. C. Ruppel, D. M. Jarvie, *J. Sediment. Res.* **79**, 848 (2009).
18. R. J. Ambrose, R. C. Hartman, M. Diaz-Campos, I. Y. Akkutlu, C. H. Sondergeld, *SPE J.* **17**, 219 (2012).
19. E. Barsotti, S. P. Tan, S. Saraji, M. Piri, J.-H. Chen, *Fuel* **184**, 344 (2016).
20. T. Zhang, G. S. Ellis, S. C. Ruppel, K. Milliken, R. Yang, *Org. Geochem.* **47**, 120 (2012).
21. M. Thommes *et al.*, *Pure Appl. Chem.* **87**, 1051 (2015).
22. I. Langmuir, *The Research Laboratory of The General Electric Company*, 1361 (1918).
23. S. Brandani, E. Mangano, L. Sarkisov, *Adsorption* **22**, 261 (2016).
24. J. B. Curtis, *AAPG Bulletin* **86**, 1921, (2002).

25. J. Liu, S. Xi, W. G. Chapman, *Langmuir* **35**, 8144 (2019).
26. M. Pathak, H. Kweon, M. Deo, H. Huang, *Sci. Rep.* **7**, 12530 (2017).
27. S. Tesson, A. Firoozabadi, *J. Phys. Chem. C* **123**, 29173 (2019).
28. S. S. Cunniff *et al.*, *Langmuir* **38**, 15540 (2022).
29. L. Michels *et al.*, *Sci. Rep.* **5**, 8775 (2015).
30. J.-H. Chen, S. Althaus, C. Liu, M. Boudjatit, paper presented at the SCA2023, Abu Dhabi, UAE, Oct. 9-12, 2023.
31. B. Nicot *et al.*, *Magn. Reson.* **3**, 125 (2022).
32. D. L. Luffel, F. K. Guidry, (1992).
33. C. Straley, D. Rossini, H. Vinegar, P. Tutunjian, C. Morriss, *The Log Analyst* **38**, (1997).
34. R. Span, W. Wagner, *J. Phys. Chem. Ref. Data* **25**, 1509 (1996).
35. A. Abragam, *The Principles of Nuclear Magnetism*. (Clarendon Press, London, 1961).
36. F. Bloch, W. W. Hansen, M. Packard, *Physical Review* **69**, 127 (1946).
37. E. W. Lemmon, I. H. Bell, M. L. Huber, M. O. McLinden, *NIST Standard Reference Database 23: Reference Fluid Thermodynamic and Transport Properties-REFPROP, Version 10.0*, (2018).

Appendix A: Estimation of total surface area in micro-/nano-porous rocks

A1. Pore surface area in a simple uniform matrix solid

In order to estimate the total pore surface area in rocks, we first consider the simplest model, that all the pores are spherical voids in a solid matrix, instead of a traditional model of packing solid spheres as matrix. For a rock with total volume V , assuming it has a porosity ϕ formed from n number of uniform spherical pores of radius r , we have

$$\phi = n \cdot 4\pi r^3 / 3V \quad (\text{A1})$$

The total surface of the pores is

$$s = n \cdot 4\pi r^2 \quad (\text{A2})$$

Calculate n from Eq. (A1) and insert into Eq. (A2) we have

$$s = 3\phi v / r \quad (\text{A3})$$

Eq. (A3) can be expressed in terms of material mass m and bulk density ρ as

$$s = \frac{3\phi m}{r\rho} \quad (\text{A4})$$

The bulk density ρ relates with porosity ϕ and matrix (grain) density ρ_m

$$\rho = (1 - \phi)\rho_m \quad (\text{A5})$$

Then we have

$$s = \frac{3\phi m}{r(1 - \phi)\rho_m} \quad (\text{A6})$$

From Eq. (A6), the surface area increases inversely proportional to the pore size. Fig. A1 is the plot of pore surface area according to the pore radius for rocks with grain density 2.65 g/cm^3 , the density of pure sand. The trend and dependence are similar for carbonate rocks except the grain density should use 2.71 g/cm^3 . It is obvious from Fig. A1 that the pore surface area in a rock significantly depends on the porosity and pore size. For traditional sandstone and carbonate with pore radius at the scale of $1 \mu\text{m}$ or larger, the total pore surface area is less than $0.5 \text{ m}^2/\text{g}$. When the pore radius approach 10 nm , the surface area is more than $10 \text{ m}^2/\text{g}$, which certainly contributes and sometime dominate some properties of the sample.

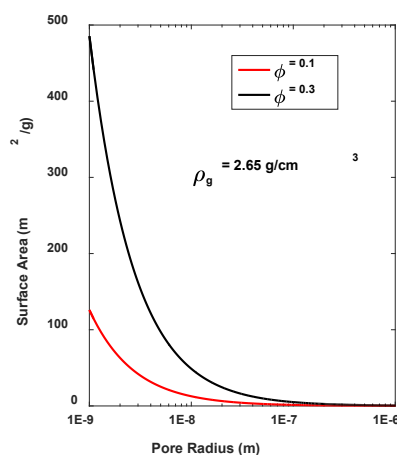


Fig. A1. A pore size dependent total pore surface for rock with uniform spherical pores and grain density 2.65 g/cm^3 .

A2. Pore surface in organic-rich source rocks

For organic-rich source rock shales, for simplicity, we assume the porosity in the inorganic mineral is negligible; thus, all the pores are in kerogen. This is true for many unconventional reservoirs where pores in kerogen dominate the total porosity.

For fractional volume of matrix V_m and kerogen V_k , we have

$$V_m + V_k = 1 \quad (\text{A7})$$

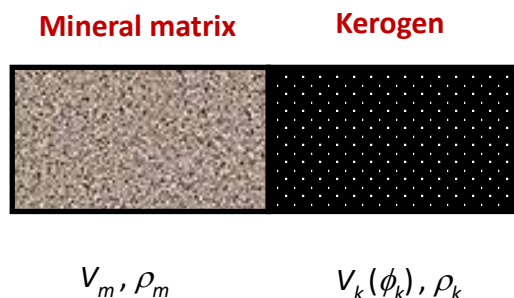


Fig. A2. Compositional scheme of shale with all the pores in kerogen

We assume we know the following parameters for the shales:

- the percent weight of kerogen f
- kerogen grain density ρ_k
- mineral grain density ρ_m

- kerogen porosity ϕ_k

Note the total porosity, with current assumptions, is

$$\phi = \phi_k \cdot v_k \quad (\text{A8})$$

The kerogen weight percent can be expressed as

$$f = \frac{(1 - \phi_k)V_k\rho_k}{(1 - \phi_k)V_k\rho_k + V_m\rho_m} \quad (\text{A9})$$

Insert Eq. (A7) into Eq. (A9), we obtain

$$V_k = \frac{f\rho_m}{(1 - f)(1 - \phi_k)\rho_k + f\rho_m} \quad (\text{A10})$$

Now we calculate the surface area in shale, assuming kerogen is the only porosity resource. In this case, the bulk density of shale is

$$\rho = (1 - \phi_k)V_k\rho_k + (1 - V_k)\rho_m \quad (\text{A11})$$

Insert Eq. (A10) into Eq. (A11)

$$\rho = \frac{(1 - \phi_k)\rho_k\rho_m}{(1 - f)(1 - \phi_k)\rho_k + f\rho_m} \quad (\text{A12})$$

From Eq. (A8) and Eq. (A10), we have the total porosity

$$\phi = \frac{\phi_k f \rho_m}{(1 - f)(1 - \phi_k)\rho_k + f\rho_m} \quad (\text{A13})$$

Insert Eqs. (A12) and (A13) into Eq. (A4), we obtain

$$s = \frac{3f\phi_k m}{r(1 - \phi_k)\rho_k} \quad (\text{A14})$$

Eq. (A14) is similar to Eq. (A6), except now it depends on the property of kerogen. The total surface is plotted vs the pore radius in Figure 2.